Apolipoprotein E–low density lipoprotein receptor interaction: influences of basic residue and amphipathic α-helix organization in the ligand

Mohamed Zaiou,* Kay S. Arnold,† Yvonne M. Newhouse,† Thomas L. Innerarity,†,§ Karl H. Weisgraber,†,§ Mark L. Segall,* Michael C. Phillips,* and Sissel Lund-Katz[1,*]

Biochemistry Department,* M. C. P. Hahnemann University, Philadelphia, PA 19129; and the Gladstone Institute of Cardiovascular Disease† and Cardiovascular Research Institute and Department of Pathology,§ University of California, San Francisco, CA 94140

Abstract **Conserved lysines and arginines within amino acids 140–150 of apolipoprotein (apo) E are crucial for the interaction between apoE and the low density lipoprotein receptor (LDLR). To explore the roles of amphipathic α-helix and basic residue organization in the binding process, we performed site-directed mutagenesis on the 22-kDa fragment of apoE (amino acids 1–191). Exchange of lysine and arginine at postions 143, 146, and 147 demonstrated that a positive charge rather than a specific basic residue is required at these positions. Consistent with this finding, substitution of neutral amino acids for the lysines at positions 143 and 146 reduced the binding affinity to about 30% of the wild-type value. This reduction corresponds to a decrease in free energy of binding of ~600 cal/mol, consistent with the elimination of a hydrogen-bonded ion pair (salt bridge) between a lysine on apoE and an acidic residue on the LDLR. Binding activity was similarly reduced when K143 and K146 were both mutated to arginine (K143R + K146R), indicating that more than the side-chain positive charge can be important. Exchanging lysines and leucines indicated that the amphipathic α-helical structure of amino acids 140–150 is critical for normal binding to the low density lipoprotein receptor.**—Zaiou, M., K. S. Arnold, Y. M. Newhouse, T. L. Innerarity, K. H. Weisgraber, M. L. Segall, M. C. Phillips, and S. Lund-Katz. **Apolipoprotein E–low density lipoprotein receptor interaction: influences of basic residue and amphipathic α-helix organization in the ligand.** ***J. Lipid Res.*** **2000.** 41: **1087–1095.**

Supplementary key words amphipathic α helix • receptor binding domain of apo E • apolipoprotein E • receptor–ligand interaction • arginine and lysine residues • salt bridge • low density lipoprotein receptor • site-directed mutagenesis

Apolipoprotein E (apoE) is a high-affinity ligand for several hepatic lipoprotein receptors, including the low density lipoprotein receptor (LDLR) and the LDLR-related protein, and for cell surface heparan sulfate proteoglycans (1, 2). Through its ability to bind to these receptors, apoE mediates lipid metabolism and cholesterol homeostasis. This role is critical. ApoE-deficient humans (3, 4) and mice (5, 6) develop severe plasma retention of chylomicron remnants. Defective binding of apoE to these receptors results in the accumulation of cholesterol-rich lipoprotein particles in the plasma and is a cause of type III hyperlipoproteinemia, a genetic disorder characterized by elevated plasma cholesterol and triglyceride levels and accelerated coronary artery disease (7). Most of the mutations in apoE responsible for defective binding involve amino acid substitutions within the region of amino acids 136–150 (8–10). Mutants with neutral amino acid substitutions for lysine and arginine at positions 142, 145, and 146 bind defectively to the LDLR (1). Site-directed mutagenesis of basic amino acids in the 136–150 region also results in defective LDLR binding (11). Thus, this region appears to be important in the binding process.

The secondary structure of apoE predicted by the Chou–Fasman algorithm (12, 13) includes an α helix between residues 131 and 150 (1, 14). The crystal structure of the N-terminal fragment (residues 1–191) also contains an α-helical domain (15). The binding of apoE to the LDLR is thought to involve electrostatic interaction between the basic receptor-binding domain of apoE and acidic, disulfide-rich repeats of the LDLR (1). However, high-resolution structural information to confirm this suspicion is not available.

The clustering of basic arginines and lysines in region 140–150 of apoE is important for receptor binding (16). However, methylation of lysine residues reduces receptor

Abbreviations: apo, apolipoprotein; DMPC, dimyristoylphosphatidylcholine; GdnHCl, guanidine hydrochloride; IC_{50}, concentration for 50% inhibition; IPTG, isopropyl-β-D-thiogalactopyranoside; LB, Luria–Bertani; LDLR, low density lipoprotein receptor; OD, optical density; PCR, polymerase chain reaction; SDS-PAGE, sodium dodecyl sulfate-polyacrylamide gel electrophoresis.

[1] To whom correspondence should be addressed at Joseph Stokes Jr. Research Institute, The Children's Hospital of Philadelphia, Abramson Bldg. Rm. 302E, 3516 Civic Center Blvd., Philadelphia, PA 19104-4318.

binding even though the side chain positive charge is retained (17), indicating that factors other than a positive charge are important. Moreover, the effects of steric fit, positive charge distribution, and any specific roles of arginine and lysine residues are not understood. To elucidate the molecular details of the apoE–LDLR interaction, we introduced a series of mutations into the human apoE3 gene. All mutants were generated from a cDNA that encodes only the 22-kDa N-terminal region of apoE3 (residues 1–191). This fragment was chosen because it contains the LDLR-binding domain (18, 19), because its binding to the LDLR is similar to that of full-length apoE3, and because its yield is greater than that of full-length apoE when expressed in *Escherichia coli*. In addition, the crystal structure of this fragment in the lipid-free state has been solved, and high-resolution structural information is available (15). The mutants were designed to address three issues about the receptor-binding domain (residues 140–150): *i*) the influence of the net charge of the basic amino acid residues on the energetics of the apoE–LDLR interaction, *ii*) the role of the amphipathicity and orientation of the α helix, and *iii*) the relative functions of arginine and lysine residues. Our findings suggest that the amphipathic α-helical structure of region 140–150 of apoE3 is required for normal receptor binding. Lysines and arginines are crucial for this interaction, and despite their similarities in charge, interchange of these residues can disrupt binding to the LDLR.

MATERIALS AND METHODS

Materials

Bacteriological media were obtained from Difco Laboratories (Detroit, MI). The prokaryotic expression vector pET21 and the competent *E. coli* strain BL21(DE3) were purchased from Novagen (Madison, WI). Competent *E. coli* DH5α and nucleotides were purchased from GIBCO-BRL (Gaithersburg, MD). *Pfu* DNA polymerase was obtained from Stratagene (La Jolla, CA). Restriction enzymes and calf intestinal alkaline phosphatase were purchased from New England BioLabs (Beverly, MA). Isopropyl-β-D-thiogalactopyranoside (IPTG), 2-mercaptoethanol, aprotinin, and ampicillin were purchased from Sigma (St. Louis, MO). Guanidine-HCl (GdnHCl) was obtained from ICN Pharmaceuticals (Costa Mesa, CA). Oligonucleotides and DNA purification kits were purchased from Oligos Etc. (Wilsonville, OR) and Qiagen (Chatsworth, CA), respectively. Dimyristoylphosphatidylcholine (DMPC) was obtained from Avanti Polar Lipids (Birmingham, AL).

Mutagenesis and construction of apoE plasmids

The expression vectors containing various mutations in the human apoE3 cDNA encoding the N-terminal fragment (residues 1–191, 22 kDa) were constructed as described previously (20). Mutagenic primers were used to introduce the mutation, stop codons, and appropriate restriction sites. The preparation of plasmid DNA and purification of DNA and of DNA fragments amplified by polymerase chain reaction (PCR) using *Pfu* DNA polymerase were performed with a QIAEX II gel extraction kit (Qiagen).

ApoE3-22 kDa mutants (K146R + R147K, K143R, K143A, K143R + K146R, L144R + R145L, L141K + K143L + K146L + L148K, and K146R) were constructed by site-directed mutagenesis, using the pET-21-apoE3-22 kDa template and sense/antisense primer pairs shown in **Table 1**. In the first round of PCR, the sequences upstream and downstream of the mutation were amplified separately with the pET-a-21-apoE3 plasmid template and the sense/end primer pairs and antisense/start primer pairs, respectively. The presence of the mutation was confirmed by DNA sequencing of double-stranded DNA (DNA Analysis Core Facility, M. C. P. Hahnemann University, Philadelphia, PA). All plasmids used for transfection were purified with the Qiagen plasmid kit.

TABLE 1. Details of oligonucleotide primers for site-directed mutagenesis[a]

Primer	Nucleotide Sequences (5′→3′)	Mutation
Start	*ggaagagtatgcatatg*AAGGTTGAACAGGCT	
End	*attggatcctta*CCGCACGCGGCCCTGTTC	
Sense	CTTGCGCAAGCTGCGT**CGGAAG**CTCCTCCGCGATGCCG	K146R + R147K
Antisense	CGGCATCGCGGAGGAG**CTTCCG**ACGCAGCTTGCGCAGG	
Sense	TCCCACCTGCGC**CGG**CTGCGT**CGG**CGGCTCCTCCGC	K143R + K146R
Antisense	GCGGAGGAGCCG**CCG**ACGCAG**CCG**GCGCAGGTGGGA	
Sense	CACCTGCGCAAG**CGGCTT**AAGCGGCTC	L144R + R145L
Antisense	GAGCCGCTT**AAGCCG**CTTGCGCAGGTG	
Sense	CACCTGCGCAAG**CGGCTT**AAGCGGCTC	K143R
Antisense	GAGCCGCTT**AAGCCG**CTTGCGCAGGTG	
Sense	CACCTGCGCAAG**CGGCTT**AAGCGGCTC	K143A
Antisense	GAGCCGCTT**AAGCCG**CTTGCGCAGGTG	
Sense	CACCTGCGCAAG**CGGCTT**AAGCGGCTC	K146R
Antisense	GAGCCGCTT**AAGCCG**CTTGCGCAGGTG	
Sense	GCCTCCCAC**AAG**CGC**CTG**CTGCGT**CTG**CGG**AAG**CTCCGCGAT	L141K + K143L + K146L + L148K
Antisense	ATCGCGGAG**CTT**CCG**CAG**ACGCAG**CAG**GCG**CTT**GTGGGAGGC	

[a] The codons for the substituting amino acid residue are underlined. The bases that have been changed are in bold face. Each pair of oligonucleotides (sense and antisense) was used to generate primary PCR products with overlapping complementary ends containing the mutation; for these reactions the external oligos start primer or end primer were also used. These were then combined as templates for a secondary PCR employing start and end primers to generate the full-length cDNA containing the mutation of interest. Start and end primers were designed to introduce specific restriction sites (indicated by lower-case italics) into the amplified products.

Overexpression of apoE in *Escherichia coli*

The plasmids containing the cDNA of the various apoE3-22 kDa mutants were transformed into protease-deficient *E. coli* strain BL21(DE3). An overnight culture of each mutant in Luria–Bertarni (LB) broth supplemented with ampicillin (100 μg/mL) was used to inoculate a 6-L culture in LB medium. The culture was grown at 37°C with constant shaking (series 25 incubator/shaker; New Brunswick Scientific, Edison, NJ) until its absorbance reached 0.5 OD at 600 nm, and expression was induced by adding IPTG to a final concentration of 0.4 mM. The expression was continued for 2.5 h, and the cells were harvested by centrifugation at 4,000 rpm for 20 min at 4°C in a J6 rotor (Beckman, Palo Alto, CA). The cells were resuspended in 30 mL of ice-cold extraction buffer (150 mM NaCl, 20 mM Na_2HPO_4, 25 mM EDTA, 2 mM phenylmethylsulfonyl fluoride, 1% Trasylol [aprotinin], 0.1% 2-mercaptoethanol, pH 7.4). The suspension was sonicated on ice with a sonifier cell disruptor 350 (Branson Ultrasonics, Danbury, CT) fitted with a ½-inch tip for three cycles of 1 min on and 2 min off. Bacterial debris was removed by centrifugation at 40,000 *g* for 20 min at 4°C.

For mutants expressed as soluble proteins in the cytoplasm of the *E. coli*, solid GdnHCl and 2-mercaptoethanol were added to the supernatant to final concentrations of 7 M and 1%, respectively. The mixture was incubated at 4°C overnight, insoluble material was removed by centrifugation for 10 min at 40,000 *g*, and the supernatant containing the recombinant proteins was recovered for further purification.

The L141K + K143L + K146L + L148K mutant was expressed in the insoluble fraction. After sonication, the insoluble material containing apoE was pelleted by centrifugation. Proteins were solubilized from the pellet at 4°C by adding 30 mL of a solution containing 7 M GdnHCl, 150 mM NaCl, 20 mM Na_2HPO_4, 25 mM EDTA, 0.1% 2-mercaptoethanol, pH 7.4. Insoluble material was removed by centrifugation for 10 min at 40,000 *g*, and the recombinant protein in the supernatant was recovered by gel-filtration chromatography as described below.

Purification of apoE

The various apoE3-22 kDa variants were separated from the *E. coli* extract by fast-performance liquid chromatography using a combination of gel-filtration, ion-exchange, and affinity techniques. First, the supernatant was applied to a Sephacryl S300 column (200 × 2.6 cm, 1-mL/min flow rate) previously equilibrated with a buffer containing 4 M GdnHCl, 0.1 M Tris-HCl (pH 7.4), 1 mM EDTA, and 0.1% 2-mercaptoethanol. ApoE was eluted with the same buffer, and the elution profile was determined by monitoring the absorbance of the effluent at 280 nm. Protein samples were analyzed for purity by sodium dodecyl sulfate–polyacrylamide gel electrophoresis (SDS-PAGE) using 8–25% Phast gels (Amersham Pharmacia Biotech, Piscataway, NJ) at each stage of the procedure. Fractions (12.5 mL) containing apoE were pooled and extensively dialyzed against 20 mM NH_4HCO_3. After dialysis, the protein samples were lyophilized and solubilized in 0.1 M NH_4HCO_3, pH 7.4. ApoE was then applied to a 5 × 16 cm Q-Sepharose ion-exchange column equilibrated with 50 mL of buffer A (6 M urea, 20 mM Tris-HCl, pH 7.4). Bound apoE was eluted by applying a 0–1 M NaCl gradient (buffer B: 6 M urea, 1 M NaCl, 20 mM Tris-HCl, pH 7.4). The fractions containing apoE were pooled, dialyzed against 25 mM NH_4HCO_3, pH 8.0, and passed through three heparin columns (HiTrap [1.5 × 1.6 cm]; Amersham Pharmacia Biotech). The column was washed with 25 mM NH_4HCO_3, pH 8.0, to remove unbound proteins, and apoE was eluted with 750 mM NH_4HCO_3, pH 8.7. The mass of apoE was quantitated by the method of Lowry *et al.* (21). The purity of apoE preparations was assessed by SDS-PAGE. The apoE3-22 kDa variants were >95% pure.

Preparation of apoE3-22 kDa•DMPC complexes

The various apoE3-22 kDa variant proteins were mixed with DMPC vesicles at a ratio of 1:3.75 (protein–DMPC, by weight) and isolated by KBr density gradient ultracentrifugation as described previously (22, 23). Briefly, the desired amount of DMPC was dried from a chloroform–methanol solution under nitrogen in a 15-mL tube. The residue was redissolved in 1–2 mL of benzene, frozen, and lyophilized. Lipids were sonicated in a buffer containing 0.15 M NaCl, 10 mM disodium EDTA, and 1 mM Tris-HCl, pH 7.6. The slightly translucent solution of DMPC vesicles was then centrifuged at low speed and kept at room temperature. The appropriate amount of apoE dissolved in 0.1 M NH_4HCO_3, pH 8.1, was added to the tube in the presence of 2-mercaptoethanol (at 0.5 μl/100 μg of protein), and the mixture was recycled three times through the gel–liquid crystal transition temperature of the DMPC (23.5°C) by warming to 37°C and cooling on ice, taking 15 min for each cycle. The DMPC·apoE3-22 kDa complexes were separated from uncomplexed protein and lipid by density gradient centrifugation. A linear KBr salt gradient (d 1.006–1.21 g/mL) was prepared in polyallomer tubes (Beckman Instruments). The lipid–protein complexes were layered on top of the gradient and centrifuged in an SW-55 rotor at 15°C for 20 h (369,000 *g*). The majority of the lipid–protein complex was removed from collected fractions in the density range of 1.09–1.10 g/mL. These fractions were pooled and dialyzed against saline–EDTA and stored at 4°C. The apoE3-22 kDa·DMPC discoidal complexes were sized by negative-stain electron microscopy (24) with a JEOL (Tokyo, Japan) 100CXII electron microscope.

Circular dichroism spectroscopy

Each apoE3-22 kDa variant was solubilized in 6 M GdnHCl containing 1% 2-mercaptoethanol for 24 h and renatured by dialysis against 10 mM phosphate buffer, pH 7.0, overnight with three changes of the buffer. The α-helix content of the various apoE preparations was determined from the M ellipticity at 222 nm ($[\theta_{222}]$) by established procedures (23, 25). The thermal denaturation was monitored by the decrease in α-helix content with increasing temperature. $[\theta_{222}]$ was recorded every 0.1°C as the temperature of a 500-μg/mL solution of apoE in phosphate buffer was increased continuously from 10 to 90°C at 1°C/min. A 0.1-cm path length, jacketed quartz cuvette was used in a JASCO (Tokyo, Japan) J600 spectropolarimeter equipped with a temperature control and interfaced with a Pentium computer. The spectropolarimeter was calibrated with *d*-10-camphorsulfonic acid. The temperature inside the cuvette was measured continuously with a calibrated thermocouple. The midpoint temperature of the sigmoidal α-helix melting curve was obtained by fitting the $[\theta_{222}]$ values at each temperature in the range 10–90°C to the Boltzmann equation for a sigmoidal curve describing a two-state unfolding process. The Van't Hoff enthalpy for the transition was calculated from the temperature dependence of the equilibrium constant for the unfolding, as described previously (26).

LDL receptor binding assay

The binding of apoE3-22 kDa·DMPC complexes to the LDLR was measured in a competitive binding assay with ^{125}I-labeled LDL, as described previously (27). LDL were isolated from the plasma of normal fasting subjects by sequential ultracentrifugation and radiolabeled by the iodine monochloride method (28). Normal human skin fibroblasts were plated at 3.5×10^4 cells/dish 1 week before the experiment. On day 5, the cells were placed in medium containing 10% lipoprotein-deficient serum. On day 7, the cells were incubated at 4°C for 2 h in medium containing ^{125}I-labeled LDL (2 μg/mL) and various concentrations

of apoE3-22 kDa·DMPC complexes. The concentration (IC_{50}) of apoE required to give 50% inhibition of the binding of ^{125}I-labeled LDL to the cells was determined.

RESULTS

Expression and isolation of recombinant apoE3 proteins

Full-length apoE3 (34 kDa) and the apoE3-22 kDa amino-terminal fragment bind equally to the LDLR when complexed with DMPC (29), and the LDLR-binding activities of the bacterially produced molecules are essentially identical to that of plasma-derived apoE3 (30). On the basis of these findings and because higher yields of the 22-kDa fragment were obtained, the receptor-binding studies were conducted with this fragment. We sought to explore the role of basic residue organization in the receptor-binding domain (residues 136–150) of the apoE3 molecule. We generated a series of mutants of the 22-kDa fragment (residues 1–191) of apoE3 to address three specific issues. K146Q and K143A were studied to assess the role of the net charge of the basic amino acid residues. L144R + R145L and L141K + K143L + K146L + L148K were studied to assess the role of the amphipathicity of the α-helix structure (**Fig. 1A–C** and **Fig. 2**). K143R, K146R, K143R + K146R (Fig. 1D), and K146R + R147K were studied to assess the functions of arginines and lysines. Except for L141K + K143L + K146L + L148K, which was recovered in the insoluble fraction presumably as inclusion bodies, all of the mutants were recovered in the soluble fraction of sonicated bacteria.

Physical characterization of apoE3 mutants

To ensure that the point mutations did not change the overall structure of the 22-kDa molecule, some structural properties of the mutant proteins were compared with those of the wild-type molecule. To ascertain whether the amino acid substitutions in apoE3-22 kDa resulted in conformational changes, the α-helix contents and the melting temperatures were measured by circular dichroism (**Table 2**). In the lipid-free state, the α-helix content of all the mu-

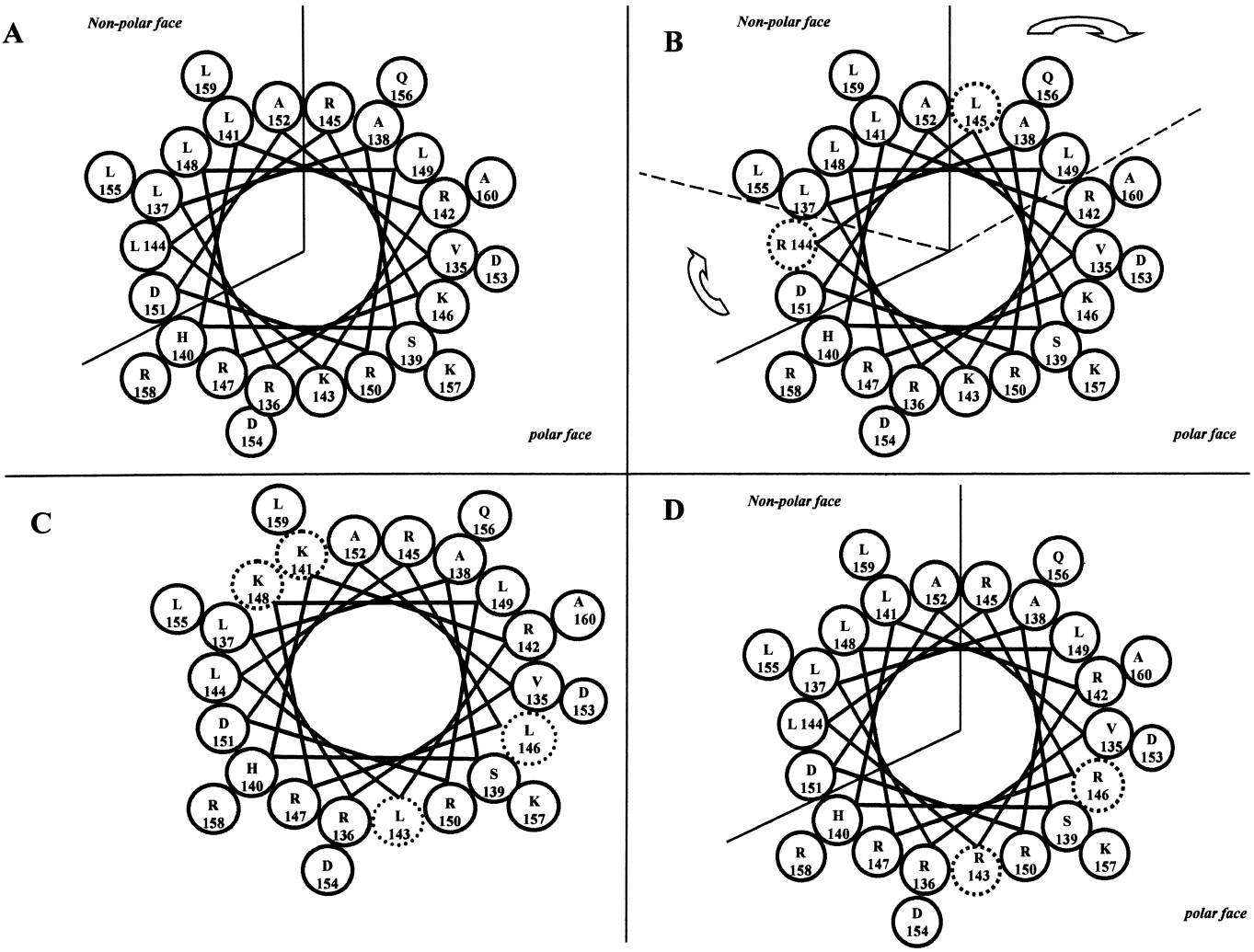

Fig. 1. Helical wheel representation of human apoE3 residues 136–160. (A) Wild type; (B) mutant L144R + R145L; (C) mutant L141K + K143L + K146L + L148K; (D) mutant K143R + K146R. Solid lines show the boundary of the polar and nonpolar faces of the amphipathic α helix. The dashed lines in (B) show the change in orientation of the polar and nonpolar faces due to the substitution of L144 and R145. Dashed circles indicate the mutated amino acids.

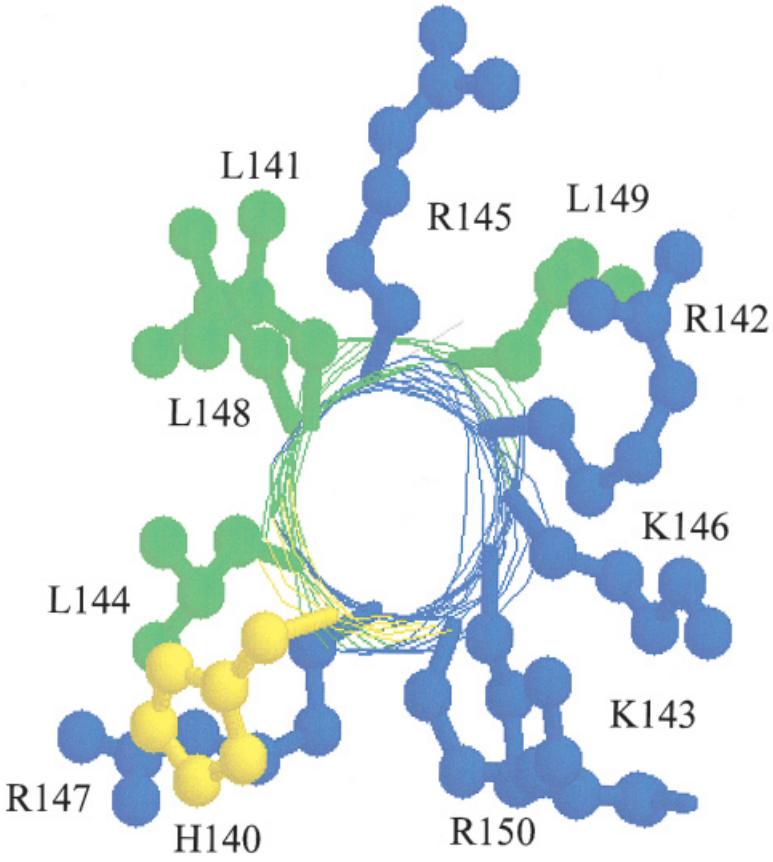

Fig. 2. End view of the amphipathic α-helix formed by residues 140–150 in the 4-helix bundle structure of the lipid-free 22-kDa fragment of apoE3 (cf. Fig. 1A). The crystal structure coordinates are from ref. 15 and the picture is drawn with Rasmol. The α-helix backbone is shown as strands and the amino acid sidechains are drawn as ball and sticks. Basic K and R residues are shown in blue and nonpolar L residues are shown in green. H140 is shown in yellow.

tants was ~50%. These values are in agreement with data obtained by circular dichroism (31). When the apoE3-22 kDa molecule was complexed with DMPC, the α-helix content increased 15–20%. Except for L141K + K143L + K146L + L148K, the mutations did not significantly alter the average secondary structure of the molecule. Most of the mutants had approximately the same stabilities as reflected by their thermal denaturation characteristics (Table 2) (melting temperature, 55 ± 2°C; Van't Hoff enthalpy of denaturation, 28 ± 2 kcal/mol); L141K + K143L + K146L + L148K had a significantly lower melting temperature (~30°C) and enthalpy of denaturation (23 kcal/mol). The helical hydrophobic moments confirm that this mutant had lower amphipathicity than the others (Table 2). The apoE3-22 kDa variants also formed discoidal apoE·DMPC complexes of similar size (major diameters in the range of 15–17 nm). The less stable mutant, L141K + K143L + K146L + L148K, formed discs of the same size as the wild-type protein.

Overall, the mutants were structurally similar and the point mutations exerted only local effects, the one notable exception being L141K + K143L + K146L + L148K.

TABLE 2. Physical characteristics of apoE3-22 kDa mutants

Apo E3-22 kDa Variant	% α Helix[a]		Helical Hydrophobic Moment[b] (kcal/mol)	Tm (°C)[c]	ΔH_{VH} (kcal/mol)[c]
	− Lipid	+ DMPC			
Wild type	53	68	0.47	57	28
K143A	51	71	0.38	55	30
K146Q	51	75	0.44	55	29
L144R + R145L	52	70	0.54	58	30
L141K + K143L + K146L + L148K	44	58	0.09	32	23
K143R	46	75	0.52	54	28
K146R	51	70	0.53	53	27
K146R + R147K	54	71	0.52	56	28
K143R + K146R	51	72	0.58	54	26

[a] Determined from molar ellipticities at 222 nm (±5%).

[b] Calculated for residues 140–150 in an α helix as described previously (32) using a consensus hydrophobicity scale (33).

[c] The midpoint temperature (T_m) (±2°C) and Van't Hoff enthalpy (ΔH_{VH}) (±2 kcal/mol) were measured as described in Materials and Methods by monitoring thermal denaturation of lipid-free apoE3-22 kDa through changes in molar ellipticity at 222 nm.

Thus, the discoidal complexes used to study binding to the LDLR were of similar size and composition; the stoichiometry was ~100/1 mol/mol DMPC/apoE3-22 kDa. Particle volumes, calculated from the particle dimensions determined by electron microscopy, lipid–protein stoichiometries, and partial specific volumes (25) indicated that each discoidal complex contained about 6 apoE3-22 kDa molecules.

LDLR binding of apoE3-22 kDa variants

In contrast to its lipid-free state, apoE3-22 kDa complexed to DMPC can bind to the LDLR (29). To assess the affinities of the apoE3-22 kDa wild-type and mutant molecules for the LDLR, we compared their abilities to displace ^{125}I-labeled LDL from the LDLR on normal human fibroblasts (**Fig. 3**). The mutants displayed different affinities (**Table 3**). Substitution of a neutral for a basic amino acid in mutants K143A and K146Q did not alter the α-helical structure of apoE3-22 kDa complexed with DMPC but did reduce LDLR binding to 25–30% of the wild-type value. This reduction was independent of amino acid side chain size; substituting alanine or glutamine for lysine gave the same reduction. These results indicate that the positive charges are critical for LDLR binding and that removing one basic amino acid decreases the binding (see ref. 11). To examine the requirement for amphipathicity in the α-helical domain of residues 140–150, lysines at positions 143 and 146 were replaced with leucines, and the leucines at positions 141 and 148 were substituted with lysines to give mutant L141K + K143L + K146L + L148K. These substitutions disrupted the amphipathicity of the α helix (Fig. 1C and Table 2; see refs. 32 and 33), while the net positive charge remained constant. This mutant retained the ability to form discs when complexed with DMPC, but it could not bind to the LDLR (Table 3). Mutations L144R + R145L did not affect the binding activity, suggesting that the relative positioning of the polar and nonpolar faces of the amphipathic α helix (Fig. 1B) is not critical. To examine the relative roles of arginine and lysine residues within domain 140–150, the positions of several of these residues were exchanged. The mutations K146R + R147K had no effect on receptor-binding affinity (Table 3). The exchanges K143R, K146R, and K143R + K146R caused distinctly different effects. K143R and K146R had full binding activity. However, K143R + K146R had reduced binding activity (31 ± 8% of the wild-type), although the number of basic residues was the same as in the wild-type protein.

TABLE 3. LDLR binding activity of apoE3-22 kDa mutants

Apo E3-22 kDa Variant	Relative Affinity for LDL-R (%)[a]
Wild type	100
K143A	25 ± 5
K146Q	30 ± 5
L144R + R145L	100
L141K + K143L + K146L + L148K	0
K146R + R147K	100
K143R	100
K146R	100
K143R + K146R	31 ± 8[b]

[a] Calculated from the concentration (IC_{50}) of apoE in discoidal complexes with DMPC required to displace 50% of the ^{125}I-labeled LDL bound to LDLR on human fibroblasts (see Materials and Methods). The relative affinities for the apoE3-22 kDa molecules are expressed as the ratio IC_{50} (wild-type)/IC_{50} (variant); the values are the average of at least two measurements that were similar. The IC_{50} for the wild-type apoE3-22 kDa is 15 ± 5 ng/ml (0.7 nM).

[b] Mean ± SEM, n = 8.

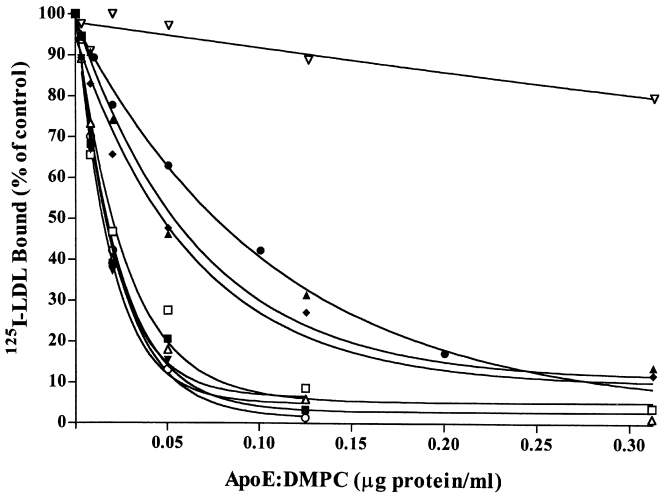

Fig. 3. Competition of different recombinant apoE3-22kDa·DMPC complexes with ^{125}I-labeled LDL for binding to the LDLR on normal human fibroblasts. (open circles) wild type; (solid triangles) K143A; (solid diamonds) K146Q; (open squares) L144R + K145L; (open inverted triangles) L141K + K143L + K146L + L148K; (solid squares) K143R; (solid inverted triangles) K146R; (open triangles) K146R + R147K; (solid circles) K143R + K146R. The competition curves are representative for each apoE3-22kDa variant. The relative affinities for the LDLR are listed in Table 3.

DISCUSSION

The interaction of apoE with lipoprotein receptors is critical for triglyceride and cholesterol metabolism in humans (1). Alignment of amino acid sequences of apoE from 10 species (16) revealed that amino acids 140–150 contain lysines at positions 143 and 146 and arginines at positions 142, 145, 147, and 150. These amino acids participate in binding to the LDLR and are conserved throughout human apoE-2, apoE-3, and apoE-4 and all species examined except the cow, where proline is substituted for arginine at position 145. This degree of conservation suggests that this domain plays a critical role in the ionic interaction of apoE with the LDLR. The molecular mechanism of the apoE–LDLR interaction cannot be elucidated until the function of each of the basic residues and the conformation of the receptor-binding domain of apoE have been determined.

Requirement for an amphipathic α helix

The three-dimensional X-ray structure of the lipid-free apoE3-22 kDa molecule has shown that a cluster of basic

amino acids is located on the polar face of helix 4 (Fig. 2) in a four-helix bundle structure (15). The receptor-binding domain in the lipid-free molecule is not recognized by the LDLR; for high-affinity binding to occur, the protein must be complexed with a lipid, such as DMPC (22, 29). The interaction with DMPC causes the four-helix bundle to open into a receptor-active conformation (16, 34). It has been suggested that the α helices of apoE in DMPC discoidal complexes are either parallel (31) or perpendicular (35) to the lipid acyl chains.

The results obtained with apoE variants generated by exchanging lysines and arginines for leucines provide insights into the role of the amphipathic α-helical structural motif. A four-point mutation (L141K + K143L + K146L + L148K) abolished the amphipathicity of the α helix-spanning residues 140–150 (see Fig. 1C and the value of the helical hydrophobic moment in Table 2), thereby destabilizing the four-helix bundle (Table 2). Nevertheless, this variant formed discoidal complexes with DMPC similar in size to those formed with the wild-type protein, despite having a 10% lower α-helix content. The loss of amphipathicity likely prevents helix 4 from interacting favorably with the DMPC acyl chains, and some unfolding of α-helix structure occurs. This reorganization abolished binding to the LDLR (Table 3), indicating that an amphipathic α-helical structure in region 140–150 is essential for receptor binding. This requirement perhaps arises from a good steric fit of the polar face of the amphipathic α helix into a pocket on the LDLR. Studies with synthetic peptides corresponding to the receptor-binding domain of apoE have also shown that an α helix is necessary for binding (36). The requirements for the orientation of the amphipathic α helix with respect to the lipid surface do not seem to be stringent. Introduction of two point mutations (L144R + R145L) altered the relative orientation of the nonpolar face of the amphipathic α helix (Fig. 1A and B) but had no effect on receptor binding (Table 3). Because the stability of the four-helix bundle formed by this variant is the same as that of the wild type, and because the α-helix content in the DMPC complex is also normal (Table 2), the functional apoE molecule seems sufficiently flexible to accommodate a helix reorientation of ~40° (Fig. 1B).

Ionic interaction between apoE and the LDLR

Consistent with the existence of electrostatic attraction between basic lysine and arginine side chains in apoE and the LDLR, a reduction in binding accompanied the loss of a positive charge. For example, defective binding was observed in a naturally occurring mutant, apoE2(K146Q) (37, 38), and in the K143A variant (11). The relative affinities of K143A and K146Q for the LDLR (~30% of wild type) also confirm the electrostatic contribution from these basic residues to the receptor–ligand interaction.

The relative affinities of the apoE variants (Table 3) reflect their abilities to compete with LDL for binding to the LDLR. The IC_{50} and the inhibition constant (K_I) can be derived from these results. The standard treatments of competitive inhibition of a Michaelis–Menten enzyme and the Scatchard analysis of receptor–ligand binding can be combined to show that $K_I = IC_{50}/(1 + F/K_d)$, where F is the concentration of free ligand. In our human fibroblast LDLR assay, F = 4 nM LDL protein, and the K_d for binding of LDL to its receptor is 2.8 nM (39). The IC_{50} for wild-type apoE3-22 kDa protein in a complex with DMPC was 0.7 nM, and the IC_{50} for K143A and K146Q was close to 2.5 nM. Knowing these IC_{50} values, we calculated K_I values for the wild-type and variant molecules of 0.3 and 1.0 nM, respectively. Because K_I is the equilibrium dissociation constant for the apoE–LDLR complex, the standard free energy of binding of the apoE sample to the LDLR is given by $\Delta G^o_b = -RT \ln(1/K_I)$. From this approach, the ΔG^o_b values for the wild-type and variant apoE3-22 kDa molecules are −12.0 and −11.4 kcal/mol, respectively. Thus, removal of a single basic residue (K143A or K146Q) reduced the favorable free energy of binding of apoE to the LDLR by ~600 cal/mol.

What does a change of 600 cal/mol in the energetics of the receptor–ligand interaction mean in terms of the nature of the intermolecular interaction? The positively charged lysines at positions 143 and 146 can potentially form ion pairs with negatively charged glutamic acid or aspartic acid residues in the LDLR. The free energy of formation of such a solvent-exposed ion pair is about −500 cal/mol (40, 41). The fact that mutation of K143 or K146 to a neutral amino acid reduces the apoE3-22 kDa–LDLR interaction by 600 cal/mol suggests that a solvent-exposed ion pair is disrupted. A buried ion pair would have a larger free energy of formation (41). It is likely that a lysine–acidic amino acid side chain interaction would also involve hydrogen bonding to form a salt bridge; the hydrogen bond would contribute significantly to the overall interaction energy (41). When bound to the LDLR, the lysines in region 140–150 of apoE are probably hydrogen bonded to glutamic acids or aspartic acids in this fashion. Methylation of the lysine ε-amino group in apoE does not affect the positive charge but reduces hydrogen bonding possibilities and abolishes binding of apoE to the LDLR (17).

Functions of lysines and arginines

To address the issue of whether the positive charge is the only factor that controls the apoE–LDLR interaction, we exchanged lysines and arginines within region 140–150 and examined the binding activities. The replacement of lysine with arginine and vice versa is generally considered to be a conservative substitution in that the net charge at neutral pH is unaltered. Consistent with the importance of conserving net charge, K143R and K146R retained full binding activity (Table 3), indicating that there is no preference between lysine or arginine at these positions. However, simultaneously mutating both lysines to arginines to create K143R + K146R reduced receptor-binding affinity to about 30% of the wild-type value (Table 3). As calculated above, this corresponds to a reduction in receptor–ligand interaction energy of about 600 cal/mol, even though the positive charge was preserved and the protein structure was identical to that of the wild-type molecule. These findings strongly suggest that conservation of

charge alone is not sufficient for high-affinity interaction of apoE with the LDLR.

Lysines and arginines are not always equivalent. The R3500K mutation in apoB-100 decreases binding to the LDLR (42). Similarly, the R42K mutation in human transforming growth factor α reduces its binding to epidermal growth factor (43), and the K203R mutation decreases the enzyme activity of cathepsin D in stimulating oligosaccharide phosphorylation (44). The effects of exchanging arginine for lysine residues in domain 140–150 of apoE are subtle; the double substitution is required before LDLR binding is affected. Because single substitutions of arginine for lysine have no effect, a complete loss of an apoE–LDLR ion pair in the double mutant (K143R + K146R) is unlikely. The arginine side chain is less flexible and longer than that of lysine. C_α–N distances are 5.64 and 6.50 Å in lysine and arginine, respectively (45). In the double mutant, the two extra arginine side chains at positions 143 and 146 are three residues apart on the polar face of the amphipathic α helix (Fig. 1A and Fig. 2). Steric interference may lead to reduced hydrogen-bonding possibilities with acidic residues on the LDLR, thereby reducing the strength of salt bridges with the LDLR.

Conclusions

The findings presented here confirm and extend qualitative measurements showing that basic residues and the net positive charge in region 140–150 of apoE are critical for interaction with the LDLR. The free energy of this receptor–ligand interaction was −12.0 kcal/mol for an apoE3-22 kDa–DMPC discoidal complex. Removal of a single basic residue in the receptor-binding domain of apoE decreased this favorable free energy of binding by about 600 cal/mol. This change decreased the affinity for the LDLR to about 30% of the wild-type value. The basic residues participate in exposed salt bridges with acidic residues on the LDLR, and hydrogen bonding is a significant part of the interaction energy. Disruption of the amphipathic nature of the α helix-spanning residues 140–150 abolishes receptor binding, indicating that this structural motif in apoE is critical for function. Exchange of lysines and arginines at a single position on the polar face of the amphipathic α helix did not significantly affect the receptor affinity of apoE. However, substitution of the lysines at positions 143 and 146 with arginines decreased the favorable free energy of binding to the LDLR to ~30% of the wild-type value, indicating that more than conservation of the positive side chain charge is involved in achieving full binding affinity. Steric effects arising from the differences between lysine and arginine side chain size and structure presumably underlie this effect.

This research was supported by NIH grants HL-56083 and HL-41633. We are indebted to Faye Baldwin, Sheila Benowitz, and Padmaja Dhanasekaran for expert technical assistance and to Gary Howard and Stephen Ordway for editorial assistance.

Manuscript received 17 December 1999 and in revised form 30 March 2000.

REFERENCES

1. Mahley, R. W. 1988. Apolipoprotein E: cholesterol transport protein with expanding role in cell biology. *Science.* **240:** 622–630.
2. Mahley, R. W. 1996. Heparan sulfate proteoglycan/low density lipoprotein receptor-related protein pathway involved in type III hyperlipoproteinemia and Alzheimer's disease. *Isr. J. Med. Sci.* **32:** 414–429.
3. Schaeffer, E. J., R. E. Gregg, G. Ghiselli, T. M. Forte, J. M. Ordovas, L. A. Zech, and H. B. Brewer, Jr. 1986. Familial apolipoprotein E deficiency. *J. Clin. Invest.* **78:** 1206–1219.
4. Mabuchi, H., H. Itoh, M. Takeda, K. Kajinami, T. Wakasugi, J. Koizumi, R. Takeda, and C. Asagami. 1989. A young type III hyperlipoproteinemic patient associated with apolipoprotein E deficiency. *Metabolism.* **38:** 115–119.
5. Zhang, S. H., R. L. Reddick, J. A. Piedrahita, and N. Maeda. 1992. Spontaneous hypercholesterolemia and arterial lesions in mice lacking apolipoprotein E. *Science.* **258:** 468–471.
6. Plump, A. S., J. D. Smith T. Hayek, K. Aalto-Setala, A. Walsh, J. G. Verstuyft, E. M. Rubin, and J. L. Breslow. 1992. Severe hypercholesterolemia and atherosclerosis in apolipoprotein E-deficient mice created by homologous recombination in ES cells. *Cell.* **71:** 343–353.
7. Mahley, R. W., and S. C. Rall, Jr. 1995. Type III hyperlipoproteinemia (dysbetalipoproteinemia): the role of apolipoprotein E in normal and abnormal lipoprotein metabolism. *In* The Metabolic and Molecular Bases of Inherited Disease, 7th ed. C. R. Scriver, A. L. Beaudet, W. S. Sly, and D. Valle, editors. McGraw-Hill, New York. 1953–1980.
8. Mann, W. A., R. E. Gregg, D. L. Sprecher, and H. B. Brewer, Jr. 1989. Apolipoprotein E-1 Harrisburg: a new variant of apolipoprotein E dominantly associated with type III hyperlipoproteinemia. *Biochim. Biophys. Acta.* **1005:** 239–244.
9. Lohse, P., W. A. Mann, E. A. Stein, and H. B. Brewer, Jr. 1991. Apolipoprotein E-4Philadelphia (Glu 13→Lys, Arg 145→Cys). Homozygosity for two rare point mutations in the apolipoprotein E gene combined with severe type III hyperlipoproteinemia. *J. Biol. Chem.* **266:** 10479–10484.
10. Mann, W. A., P. Lohse, R. E. Gregg, R. Ronan, J. M. Hoeg, L. A. Zech, and H. B. Brewer, Jr. 1995. Dominant expression of type III hyperlipoproteinemia. Pathophysiological insights derived from the structural and kinetic characteristics of Apo E-1 (Lys 146→Glu). *J. Clin. Invest.* **96:** 1100–1107.
11. Lalazar, A., K. H. Weisgraber, S. C. Rall, Jr., H. Giladi, T. L. Innerarity, A. Z. Levanon, J. K. Boyles, B. Amit, M. Gorecki, R. W. Mahley, and T. Vogel. 1988. Site-specific mutagenesis of human apolipoprotein E. Receptor binding activity of variants with single amino acid substitutions. *J. Biol. Chem.* **263:** 3542–3545.
12. Chou, P. Y., and G. D. Fasman. 1974. Conformational parameters for amino acids in helical, beta-sheet, and random coil regions calculated from proteins. *Biochemistry.* **13:** 211–222.
13. Chou, P. Y., and G. D. Fasman. 1974. Prediction of protein conformation. *Biochemistry.* **13:** 222–245.
14. Anantharamaiah, G. M., M. K. Jones, and J. P. Segrest. 1993. An atlas of the amphipathic helical domains of human exchangeable plasma apolipoproteins. *In* The Amphipathic Helix. R. M. Epand, editor. CRC Press, Boca Raton, FL. 109–142.
15. Wilson, C., M. R. Wardell, K. H. Weisgraber, R. W. Mahley, and D. A. Agard. 1991. Three-dimensional structure of the LDL receptor-binding domain of human apolipoprotein E. *Science.* **252:** 1817–1822.
16. Weisgraber, K. H. 1994. Apolipoprotein E: structure–function relationships. *Adv. Protein Chem.* **45:** 249–302.
17. Weisgraber, K. H., T. L. Innerarity, and R. W. Mahley. 1978. Role of the lysine residues of plasma lipoproteins in high affinity binding to cell surface receptors on human fibroblasts. *J. Biol. Chem.* **253:** 9053–9062.
18. Aggerbeck, L. P., J. R. Wettereau, K. H. Weisgraber, C-S. Wu, and F. T. Lindgren. 1988. Human apolipoprotein E3 in aqueous solution. II. Properties of the amino- and carboxyl-terminal domains. *J. Biol. Chem.* **263:** 6249–6258.
19. Wettereau, J. R., L. P. Aggerbeck, S. C. Rall, Jr., and K. H. Weisgraber. 1988. Human apolipoprotein E3 in aqueous solution. *J. Biol. Chem.* **263:** 6240–6248.
20. Higuchi, R. 1990. Recombinant PCR. *In* PCR Protocols: A Guide to Methods and Applications, 2nd Ed. M. A. Innis, D. H. Gelfand, J. J. Sninsky, and T. J. White, editors. Academic Press, San Diego, CA. 177–183,

21. Lowry, O. H., N. J. Rosebrough, A. L. Farr, and R. J. Randall. 1951. Protein measurement with the Folin phenol reagent. *J. Biol. Chem.* **193:** 265–275.
22. Innerarity, T. L., R. E. Pitas, and R. W. Mahley. 1979. Binding of arginine-rich (E) apoprotein after recombination with phospholipid vesicles to the low density lipoprotein receptors of fibroblasts. *J. Biol. Chem.* **254:** 4186–4190.
23. Lund-Katz, S., K. H. Weisgraber, R. W. Mahley, and M. C. Phillips. 1993. Conformation of apolipoprotein E in lipoproteins. *J. Biol. Chem.* **268:** 23008–23015.
24. Forte, T. M., and R. W. Nordhausen. 1986. Electron microscopy of negatively stained lipoproteins. *Methods Enzymol.* **128:** 442–457.
25. Sparks, D. L., M. C. Phillips, and S. Lund-Katz. 1992. The conformation of apolipoprotein A-I discoidal and spherical recombinant high density lipoprotein particles. *J. Biol. Chem.* **267:** 25830–25839.
26. Reijngoud, D. J., and M. C. Phillips. 1984. Mechanism of dissociation of human apolipoproteins A-I, A-II, and C from complexes with dimyristoylphosphatidylcholine as studied by thermal denaturation. *Biochemistry.* **23:** 726–734.
27. Arnold, K. S., T. L. Innerarity, R. E. Pitas, and R. W. Mahley. 1992. Lipoprotein–receptor interactions. *In* Lipoprotein Analysis: A Practical Approach. C. A. Converse and E. R. Skinner, editors. Oxford University Press, Oxford. 145–168.
28. Bilheimer, D. W., S. Eisenberg, and R. I. Levy. 1972. The metabolism of very low density lipoprotein proteins. I. Preliminary in vitro and in vivo observations. *Biochim. Biophys. Acta.* **260:** 212–221.
29. Innerarity, T. L., E. J. Friedlander, S. C. Rall, Jr., K. H. Weisgraber, and R. W. Mahley. 1983. The receptor-binding domain of human apolipoprotein E. Binding of apolipoprotein E fragments. *J. Biol. Chem.* **258:** 12341–12347.
30. Vogel, T., K. H. Weisgraber, M. Zeevi, H. Ben-Artzi, A. Z. Levanon, S. C. Rall, Jr., T. L. Innerarity, D. L. Hui, J. M. Taylor, D. Kanner, Z. Yavin, B. Amit, H. Aviv, M. Gorecki, and R. W. Mahley. 1985. Human apolipoprotein E expression in *Escherichia coli*: structural and functional identity of the bacterially produced protein with plasma apolipoprotein E. *Proc. Natl. Acad. Sci. USA.* **82:** 8696–8700.
31. De Pauw, M., B. Vanloo, K. H. Weisgraber, and M. Rosseneu. 1995. Comparison of lipid-binding and lecithin:cholesterol acyltransferase activation of the amino- and carboxyl-terminal domains of human apolipoprotein E3. *Biochemistry.* **34:** 10953–10960.
32. Eisenberg, D., R. M. Weiss, and T. C. Terwilliger. 1982. The helical hydrophobic moment: a measure of the amphipathicity of a helix. *Nature.* **299:** 371–374.
33. Eisenberg, D. 1984. Three-dimensional structure of membrane and surface proteins. *Annu. Rev. Biochem.* **53:** 595–623.
34. Fisher, C. A., and R. O. Ryan. 1994. Lipid binding-induced conformational changes in the N-terminal domain of human apolipoprotein E. *J. Lipid Res.* **40:** 93–99.
35. Raussens, V., C. A. Fisher, E. Goormaghtigh, R. O. Ryan, and J-M. Ruysschaert. 1998. The low density lipoprotein receptor active conformation of apolipoprotein E. *J. Biol. Chem.* **273:** 25825–25830.
36. Dyer, C. A., D. P. Cistola, G. C. Parry, and K. C. Linda. 1995. Structural features of synthetic peptides of apolipoprotein E that bind the LDL receptor. *J. Lipid Res.* **36:** 80–88.
37. Rall, S. C., Jr., K. H. Weisgraber, T. L. Innerarity, T. P. Bersot, R. W. Mahley, and C. B. Blum. 1983. Identification of a new structural variant of human apolipoprotein E E2 (Lys_{146} to Gln), in a type III hyperlipoproteinemic subject with the E3/2 phenotype. *J. Clin. Invest.* **72:** 1288–1297.
38. Smit, M., P. de Kniff, E. van der Kooij-Meijis, C. Groenendijk, A. M. J. M. van den Maagdenberg, J. A. Gevers-Leuven, A. F. H. Stalenhoef, P. M. J. Stuyt, R. R. Frants, and L. M. Havekes. 1990. Genetic heterogeneity in familial dysbetalipoproteinemia. The E2 (Lys 146→Gln) variant results in a dominant mode of inheritance. *J. Lipid Res.* **31:** 45–53.
39. Innerarity, T. L., R. E. Pitas, and R. W. Mahley. 1986. Lipoprotein-receptor interactions. *Methods Enzymol.* **129:** 542–565.
40. Lyu, P. C., P. J. Gans, and N. R. Kallenbach. 1992. Energetic contribution of solvent-exposed ion pairs to alpha-helix structure. *J. Mol. Biol.* **223:** 343–350.
41. Scholtz, J. M., H. Qian, V. H. Robbins, and R. H. Baldwin, 1993. The energetics of ion-pair and hydrogen-bonding interactions in a helical peptide. *Biochemistry.* **32:** 9668–9676.
42. Borén, J., I. Lee, W. Zhu, K. Arnold, S. Taylor, and T. L. Innerarity. 1998. Identification of the low density lipoprotein receptor-binding site in apolipoprotein B100 and the modulation of its binding activity by the carboxyl terminus in familial defective apo-B100. *J. Clin. Invest.* **101:** 1084–1093.
43. Defeo-Jones, D., J. Y. Tai, G. A. Vuocolo, R. J. Wegrzyn, T. L. Schofield, M. W. Riemen. and A. Oliff. 1989. Substitution of lysine for arginine at position 42 of human transforming growth factor-alpha eliminates biological activity without changing internal disulfide bonds. *Mol. Cell. Biol.* **9:** 4083–4086.
44. Baranski, T. J., G. Koelsch, J. A. Hartsuck, and S. Kornfeld. 1991. Mapping and molecular modeling of a recognition domain for lysosomal enzyme targeting. *J. Biol. Chem.* **266:** 23365–23372.
45. Vacca, R. A., S. Giannattasio, R. Graber, E. Sandmeier, E. Marra, and P. Christen. 1997. Active-site Arg Lys substitutions alter reaction and substrate specificity of aspartate aminotransferase. *J. Biol. Chem.* **272:** 21932–21937.